Available online at www.sciencedirect.com
SCIENCE DIRECT®
Tetrahedron
Tetrahedron 60 (2004) 1099–1106

Synthesis and characterization of β-fused porphyrin-BODIPY® dyads

Kenyu Tan,[a] Laurent Jaquinod,[a] Roberto Paolesse,[b,c] Sara Nardis,[b] Corrado Di Natale,[c,d] Aldo Di Carlo,[d] Luca Prodi,[e] Marco Montalti,[e] Nelsi Zaccheroni[e] and Kevin M. Smith[a,f,*]

[a]*Department of Chemistry, University of California, Davis, CA 95616, USA*
[b]*Dipartimento di Scienze e Tecnologie Chimiche, Università di Roma 'Tor Vergata', Via della Ricerca Scientifica, 00133 Rome, Italy*
[c]*CNR-IMM, via del Fosso del Cavaliere, 00133 Rome, Italy*
[d]*Dipartimento di Ingegneria Elettronica and INFM, Università di Roma 'Tor Vergata', Via di Tor Vergata 110, 00173 Rome, Italy*
[e]*Dipartimento di Chimica 'G. Ciamician', Università di Bologna, Italy*
[f]*Department of Chemistry, Louisiana State University, Baton Rouge, LA 70803, USA*

Received 30 October 2003; revised 24 November 2003; accepted 24 November 2003

Abstract—Novel dyads in which a porphyrin ring is directly fused through two β-pyrrolic carbons to a BODIPY® moiety have been prepared using a stepwise approach starting from the copper(II) complex of pyrrolo[2,3-*c*]-5,10,15,20-tetraphenylporphyrin. Formylation and reaction with 3,5-dimethylpyrrole afforded **8**; subsequent BF_2 complexation gave the TPP-BODIPY® dyad in reasonable yields. Demetalation in TFA/H_2SO_4 led to the corresponding free base **12**, opening the way to the subsequent preparation of the Zn complex **13**. Both **12** and **13** exhibited complex optical spectra with an intensely red-shifted Q-band. Luminescence spectra displayed a very intense band around 700 nm making these species suitable as near-IR dyes and sensors in biological media. Optical analyses of **12**, using the INDO/SCI technique, were performed to obtain information to establish the origin of the novel optical properties. These studies showed that the optical properties of **12** cannot be attributed to deformation of the molecular skeleton, but derive from the increased extension of the conjugation between the TPP and BODIPY® π-systems.

1. Introduction

The exploitation of organic compounds in electronic and optoelectronic devices is one of the most exciting and challenging themes of research, with potential for enormous improvements in the performance of such devices. The discovery of the electrical conducting properties of polyacetylene[1] by Heeger, MacDiarmid and Shirakawa, who were awarded the 2000 Nobel Prize for Chemistry, can be considered the starting point of this field of research. Since their initial report, continuous effort has been focussed on the preparation of molecules to be used as organic conducting or optical materials. New organic compounds have been successfully employed in different technological applications,[2] although several problems still confine these molecular devices to the laboratory curiosity category and prevent their introduction into a marketplace dominated by silicon-based devices. Organic compounds should have molecular properties, such as stability, optical and redox properties, tailored for the subsequent application, and it is important to control the solid state aggregation of the organic material in the solid film, which is in several cases critical for the performances of the device.[3]

The presence of a highly delocalized π-electron system in a molecule such as a porphyrin provides a variety of advantages for their application. Indeed, one of the ways to enhance the use of porphyrins in optolectronic devices is to further expand the existing π-system.[4] Porphyrins are particularly appealing because of the richness of their properties, and because expertise is available to modify these useful platforms to build more complex molecular architectures.[5] We have been involved in this field of research and have reported the preparation of porphyrin arrays, and in particular oligoporphyrin systems where the macrocycles are covalently fused at their β-pyrrolic positions,[6] and the strong electronic interaction within the macrocycles results in a unique photophysical behavior.[6b] Similar fused arrays have been proposed as molecular wires[5,7] Our attention has been focused on heterodyads, in which a porphyrin and a different chromophore are fused through their π-aromatic systems by sharing two adjacent β-carbons.[8]

Keywords: Fused porphyrins; Porphyrin dyads; BODIPY; Optical spectra; INDO/SCI theory.
* Corresponding author. Address: Office of Research and Graduate Studies, Louisiana State University, 130 David Boyd Hall, Baton Rouge, LA 70803, USA. Tel.: +1-225-578-4422; fax: +1-225-578-5983; e-mail address: kmsmith@lsu.edu

0040–4020/$ - see front matter © 2003 Elsevier Ltd. All rights reserved.
doi:10.1016/j.tet.2003.11.072

Among the different chromophores, 4,4-difluoro-4-bora-3a,4a-diaza-*s*-indacene (BODIPY®) and related dyes have been used for several applications,[9] because of their stability, high absorption and emission bands and the independence of the optical properties from the pH of the solution. BODIPY® fluorophores have strong absorption and high fluorescence quantum yields with emission maxima from 490 to 650 nm.

BODIPY® dyes were first prepared by Treibs and Kreuzer in 1968.[10] Solutions of the alkyl-substituted derivatives have a green, fluorescein-like fluorescence. When substituents that introduce additional conjugation are added to the parent molecule, both the absorption and emission spectra of the derivatives can shift to significantly longer wavelengths.[11] Hence one would expect that a BODIPY® dye that is partly conjugated with the aromatic system of a porphyrin macrocycle might result in absorption and emission spectra significantly red-shifted beyond 650 nm. Examples of dyes in which BODIPY® units are fused to benzene rings have been described,[12] but analogues directly fused to porphyrin chromophores have not. BODIPY®-molecules appended to porphyrins[13] and to 21-thia- and 21-oxa-porphyrins[14] (in which the BODIPY® units are attached via unrestricted phenylalkynyl linkers) have been reported.

The fused pyrroloporphyrin[15] represents the natural starting material for rational synthesis of new π-extended molecules in which BODIPY® and porphyrin moieties are directly fused at their β-pyrrolic positions. Herein we describe the synthesis and photophysical characterization of porphyrin-BODIPY® dyads **12** and **13**. Optical properties of **12** have been investigated by use of the INDO/SCI technique, to provide information on the spectroscopic signature of these species.

2. Experimental

2.1. General

5,10,15,20-Tetraphenylporphyrin (H_2TPP) and its metal derivatives were synthesized according to the literature.[16] The Cu and Ni complexes of 2-nitroTPP were also prepared according to the literature.[17] N_2O_4 gas was prepared by reacting HNO_3 with zinc metal.[17] Melting points were measured on a Thomas/Bristoline microscopic hot stage apparatus and are uncorrected. ^{1}H NMR spectra were obtained in deuteriochloroform solution at 300 MHz using a General Electric QE 300 spectrometer; chemical shifts are expressed in ppm relative to residual $CHCl_3$ (at 7.258 ppm) in the deuterated solvent, unless otherwise stated. All chemicals were obtained from commercial suppliers and used without further purification. THF was distilled from Na/benzophenone and toluene was distilled from calcium hydride prior to use. Elemental analyses were performed at the Midwest Microlab., Inc., Indianapolis, IN. Mass spectra (MALDI-TOF) were obtained at the Facility for Advanced Instrumentation, University of California, Davis, CA. Electronic spectra were measured in dichloromethane using a Hitachi U-2000 spectrophotometer or a Hewlett–Packard 8450A spectrophotometer (Davis) and a Perkin–Elmer Lambda 16 spectrophotometer (Bologna). Uncorrected emission and corrected excitation spectra were obtained with a Perkin–Elmer LS50 spectrofluorimeter. The fluorescence lifetimes (uncertainty, ±5%) were obtained with an Edinburgh single-photon counting apparatus, in which the flash lamp was filled with N_2. Emission spectra in a rigid, transparent 2-methylcyclohexane matrix at 77 K were recorded using quartz tubes immersed in a quartz Dewar filled with liquid N_2. Fluorescence quantum yields were determined using H_2TPP (Φ=0.11) in deaerated toluene[18] as a reference. In order to allow comparison of emission intensities, corrections for the different absorbance[19] and phototube sensitivity were performed. A correction for a difference in the refractive index was introduced when necessary.

2.1.1. Copper(II) 5,10,15,20-tetraphenyl[(2,3-c)pyrroloformyl]porphyrin (4). The β-fused-di-α-free-pyrroloporphyrin **1**[14] (0.60 g, 0.841 mmol) was dissolved in trimethylorthoformate (30 mL, 0.274 mol) and treated with TFA (30 mL, 0.393 mol). The reaction was allowed to stir under argon at 0 °C for 10 min and at room temperature for 30 min (TLC monitoring). Next, cold water was added and the mixture was stirred for 2 h before 500 mL of saturated aq. Na_2CO_3 was added and stirring was continued for another 1 h. The organic layer was then separated and was washed with H_2O twice. The title porphyrin **4** (0.522 g, 83%) was recrystallized from CH_2Cl_2/MeOH. Mp>300 °C. UV/vis λ_{max} (CH_2Cl_2) 432 nm (ε 239,000), 558 (16,700), 604 (15,300), 658 (8600). MS *m*/*z* 741.6 (M^+). Anal. calcd for $C_{47}H_{29}CuN_5O\cdot H_20$: C, 75.14; H, 4.01; N, 9.21. Found: C, 75.03; H, 4.08; N, 8.98.

2.1.2. Nickel(II) 5,10,15,20-tetraphenyl[(2,3-c)pyrroloformyl]porphyrin (5). The title compound was obtained as described above (0.312 g scale, 96%), starting from β-fused-di-α-free pyrroloporphyrin **3**. Mp>300 °C. UV/vis λ_{max} (CH_2Cl_2) 432 nm (ε 137,700), 552 (12,300), 596 (12,200), 658 (3300). ^{1}H NMR ($CDCl_3$): δ 6.14 (d, 1H, *J*=3.6 Hz), 6.95 (s, 1H), 7.68 (br, 10H), 7.78 (br, 5H), 8.08 (br, 5H), 8.14 (s, *J*=7.2 Hz, 1H), 8.51 (d, *J*=4.8 Hz, 1H), 8.60 (s, 1H), 8.66 (d, *J*=4.8 Hz, 1H), 8.73 (d, *J*=5.1 Hz, 1H), 8.80 (d, *J*=5.4 Hz), 9.83 (s, 1H). MS *m*/*z* 738.1 (M^+). Anal. calcd for $C_{47}H_{29}N_5ONi\cdot 0.5H_2O$: C, 75.53; H, 4.04; N, 9.37. Found: C, 75.96; H, 3.88; N, 9.03.

2.1.3. Copper(II) 5,10,15,20-tetraphenyldipyrrometheno-porphyrin hydrochloride (9). The formylpyrroloporphyrin **4** (98.4 mg, 0.132 mmol) was dissolved in 25 mL of CH_2Cl_2 and degassed with argon for 5 min. 2,4-Dimethylpyrrole (0.02 g, 0.210 mmol) was added to the reaction mixture followed by TFA (0.20 mL, 0.261 mmol). The reaction mixture was stirred for 1 day (TLC monitoring). Washing with saturated $NaHCO_3$ afforded the unstable dipyrromethenoporphyrin free base, and is not recommended. Workup involved an aqueous work up using brine and the organic layer (CH_2Cl_2) was collected, reduced in volume (to 50 mL) using a rotary evaporator and compound **9** precipitated from solution as the hydrochloride after addition of MeOH and further concentration (97 mg, 90%). Mp>300 °C. Anal. calcd for $C_{53}H_{37}ClCuN_6$: C, 74.29; H, 4.35; N, 9.81. Found: C, 74.34; H, 4.66; N, 9.49.

2.1.4. Nickel(II) 5,1015,20-tetraphenyldipyrromethenoporphyrin hydrochloride (10). This complex was obtained (81 mg, 73%) as described above using the nickel(II) formylpyrroloporphyrin **5**. Mp>300 °C. UV/vis λ_{max} (CH_2Cl_2) 424 nm (ε 48,800), 530 (25,300), 686 (16,400). MS calcd for $C_{53}H_{36}N_6Ni$ *m/z* 814.2. Found: *m/z* 813.9 (M^+). ^1H NMRs ($CDCl_3$): δ 1.91 (s, 3H), 2.25 (s, 3H), 5.37 (s, 1H), 5.75 (s, 1H), 6.92 (d, *J*=1.8 Hz, 1H), 7.19 (s, 2H), 7.60 (m, 8H), 7.68 (s, 5H), 7.93 (m, 5H), 8.24 (d, *J*=5.1 Hz, 2H), 8.53 (d, *J*=4.5 Hz, 2H), 8.58 (d, *J*=4.2 Hz, 1H), 8.72 (d, *J*=4.8 Hz, 1H). Anal. calcd for $C_{53}H_{37}ClN_6Ni{\cdot}H_20$: C, 73.16; H, 4.52; N, 9.66. Found: C, 72.88; H, 4.98; N, 9.42.

2.1.5. Copper(II) dipyrromethenoporphyrin BF_2 complex (8). The copper(II) dipyrromethenoporphyrin hydrochloride **9** (100 mg, 0.121 mmol) was dissolved in toluene (10 mL) and degassed for 5 min. Triethylamine (0.10 mL, 0.82 mmol) and boron trifluoride etherate (0.10 mL, 0.79 mmol) were added and the reaction mixture was allowed to stir for 1 day (TLC monitoring) under an argon atmosphere. The reaction mixture was worked up with 5% HCl and water and the organic layer was collected and reduced in volume. This organic phase was then passed through a silica plug (3:1 CH_2Cl_2/cyclohexane) to remove baseline impurities. The eluent was then collected and concentrated. Upon addition of MeOH, **8** precipitated and was collected (71 mg, 65%). Mp>300 °C. MS calcd for $C_{53}H_{35}BCuF_2N_6$ *m/z* 867.2. Found: *m/z* 868.6 (M^+).

2.1.6. Metal-free dipyrromethenoporphyrin (11). A solution of **8** (0.230 g, 0.280 mmol) in 5 mL of CH_2Cl_2 was sonicated for 5 min. A mixture of TFA/2% sulfuric acid (10 mL/0.2 mL) was added and the reaction mixture was stirred vigorously for 2 min and then poured into a mixture of ice/water. The aqueous phase was extracted with CH_2Cl_2 (3×250 mL), washed with a saturated solution of $NaHCO_3$ and then with H_2O. The organic phase was evaporated and the residue was chromatographed on an alumina (Brockmann Grade V) column (eluting with CH_2Cl_2/cyclohexane 3/1). The main green band was collected and evaporated to yield compound **11** which was further recrystallized from CH_2Cl_2/cyclohexane (100.7 mg, 47%). Mp>300 °C. MS calcd for $C_{53}H_{38}N_6$ *m/z* 758.3. Found: *m/z* 759.9. ^1H NMR ($CDCl_3$): δ −2.29 (s, 2H), 2.01 (s, 3H), 2.27 (s, 3H), 5.49 (s, 1H), 5.84 (s, 1H), 6.84 (s, 1H), 7.18 (s, 5H), 7.78 (m, 5H), 8.15 (m, 10H), 8.24 (d, *J*=7.5 Hz, 2H), 8.44 (d, *J*=5.1 Hz, 2H), 8.60 (d, *J*=10.5 Hz, 1H), 8.73 (d, *J*=5.1 Hz, 1H). Anal. calcd for $C_{53}H_{38}N_6{\cdot}0.5H_2O$: C, 82.90; H, 5.12; N, 10.94. Found: C, 83.22; H, 5.17; N, 10.87.

2.1.7. Metal-free dipyrromethenoporphyrin BF_2 complex (12). Metal-free dipyrromethenoporphyrin **11** (48.9 mg, 0.0644 mmol) was dissolved in toluene (5 mL) and degassed for 5 min. Triethylamine (0.10 mL, 0.817 mmol) and boron trifluoride etherate (0.100 mL, 0.789 mmol) were added and the reaction mixture was stirred for 1 day (TLC monitoring) under an argon atmosphere. The reaction mixture was worked up with 5% HCl and H_2O and the organic layer was collected and reduced in volume. The reduced organic phase was then passed through a silica gel plug (3:1 CH_2Cl_2/cyclohexane) to remove baseline impurities. The product was observed to be unstable in solution and on an alumina TLC. The eluent was then collected and concentrated. Upon addition of MeOH, **12** precipitated (22 mg, 42%). Mp>300 °C. MS calcd for $C_{53}H_{37}BF_2N_6$ *m/z* 806.3. Found: *m/z* 806.4 (M^+). ^1H NMR ($CDCl_3$): δ −2.12 (s, 1H), 2.36 (s, 3H), 2.56 (s, 3H), 5.35 (s, 1H), 6.10 (s, 1H), 6.93 (d, *J*=1.8 Hz, 1H), 7.76 (br, 2H), 7.88 (br, 8H), 8.20 (s, 5H), 8.26 (br, 5H), 8.58 (d, *J*=5.1 Hz, 2H), 8.66 (d, *J*=4.5 Hz, 2H), 8.78 (d, *J*=4.2 Hz, 1H), 8.86 (d, *J*=4.8 Hz, 1H).

2.1.8. Zinc(II) dipyrromethenoporphyrin BF_2 complex (13). Zinc acetate (25 mg, 0.136 mmol) was added to metal-free dipyrromethenoporphyrin BF_2 complex, **12** (20 mg, 0.025 mmol) dissolved in toluene (5 mL). The reaction mixture was stirred overnight (TLC monitoring). At the end of this time the solution was pinkish-red in color. The reaction mixture was poured into H_2O and the aqueous layer was extracted with CH_2Cl_2 (2×30 mL). The organic layers were then collected and passed through a silica gel plug to remove baseline impurities. The organic layer was then reduced in volume and after addition of cyclohexane, compound **13** precipitated (15 mg, 68%). Mp>300 °C. MS calcd for $C_{53}H_{35}BF_2N_6Zn$ *m/z* 868.2. Found: *m/z* 868.2 (M^+). ^1H NMR ($CDCl_3$): δ 2.18 (s, 3H), 2.56 (s, 3H), 5.18 (s, 1H), 6.07 (s, 1H), 7.10 (d, *J*=1.8 Hz, 1H), 7.75 (br, 5H), 7.86 (br, 5H), 8.18 (m, 5H), 8.24 (br, 5H), 8.54 (d, *J*=4.8 Hz, 2H), 8.81 (d, *J*=6.6 Hz, 2H), 8.84 (s, 1H), 8.90 (d, *J*=4.8 Hz, 1H). Anal. calcd for $C_{53}H_{35}BF_2N_6Zn{\cdot}2H_20$: C, 70.25; H, 4.34; N, 9.27. Found: C, 70.06; H, 4.66; N, 9.35.

3. Results and discussion

3.1. Synthesis

The synthetic pathway leading to the formation of **8** is presented in Scheme 1. The first step is the formation of **4** from the pyrroloporphyrin **1**. The formylation reaction of pyrroles is generally carried out by the Vilsmeier reaction ($POCl_3$ and DMF); however, the Vilsmeier reagent is known to react at the β-positions of tetraarylporphyrins.[20] We carried out the reaction using TFA and trimethylorthoformate, in order to selectively functionalize the pyrrole moiety. In theory, this methodology can afford diformylated species and it has been used to prepare 2,5-diformylpyrroles[21] or 1,9-diformyldipyrromethanes from their corresponding di-α-free precursors.[22] Furthermore the TFA and $HC(OMe)_3$ system has also been used by Montforts et al.[23] to regioselectively formylate unhindered β-positions of deuteroporphyrin. In our case, the reaction of **1** with TFA/$HC(OMe)_3$ gave only one formylation product. No bis- or di-formylated derivatives were observed by mass spectrometry. The ^1H NMR spectrum confirmed that the substitution took place at the α-position of the fused pyrrole ring (the α-proton peak at 6.95 ppm integrated as one proton). Metal-free formylpyrroloporphyrin [obtained by treatment with TFA/H_2SO_4 (not shown)] is stable. Free-base pyrroleporphyrins are very unstable.[15b]

A different route for **4** is available in which the starting material is the pyrroloporphyrin *t*-butyl ester **2**. Cleavage of the *t*-butyl ester protecting group, decarboxylation of the subsequent carboxylic acid group and formylation of the

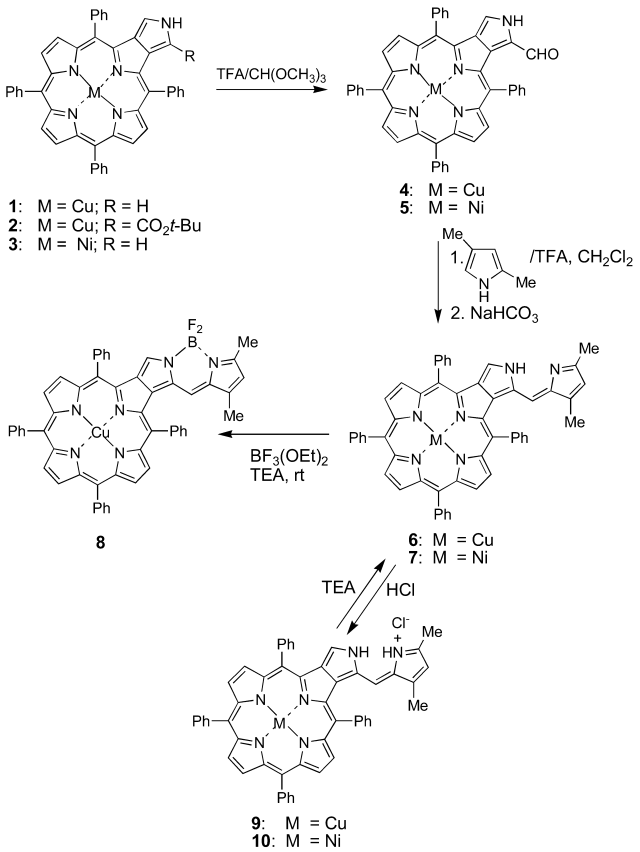

Scheme 1. Synthesis of CuTPP-BODIPY® **8**.

fused pyrrole moiety take place in a one-pot reaction. The overall yield of the reaction was somewhat lower (43%) and for this reason formylation of the α,α′-di-unsubstituted pyrroloporphyrin was preferred.

Acid-catalyzed condensation of **4** with 2,4-dimethylpyrrole gave dipyrromethenoporphyrin **6**. The reaction was quite similar to the synthesis of dipyrromethanoporphyrins obtained by condensing α-alkyl-ester pyrroloporphyrin and 5-acetoxypyrroles under slightly acidic conditions (Montmorillonite clay K-10).[15] The free base dipyrromethene derivative **6** was obtained after washing the reaction mixture with saturated $NaHCO_3$ solution. Preferably the reaction product was isolated as the protonated form **9**. The free base **6** is less stable than **9** and it was prone to decomposition over time (especially after being exposed to light and air); for this reason analytically pure compounds were characterized in their protonated forms. UV–visible spectra of **6** and **9** are reported in Figure 1. These species can be easily interconverted in solution by addition of acid or bases. It is worth mentioning that the absorption attributed to the dipyrromethene unit for **9** is similar to that observed for the BODIPY® derivative **8**, while the same band has a significant blue shift (~30 nm) in the case of **6**. In most cases, the protonated dipyrrometheno-porphyrins were characterized as the hydrochloride salts, due to anion exchange of the salt product with chloride from a brine wash. The same behavior was observed when the reaction was carried out on Ni complex **5** to give **7** and **10**.

The complexation of boron trifluoride etherate by the

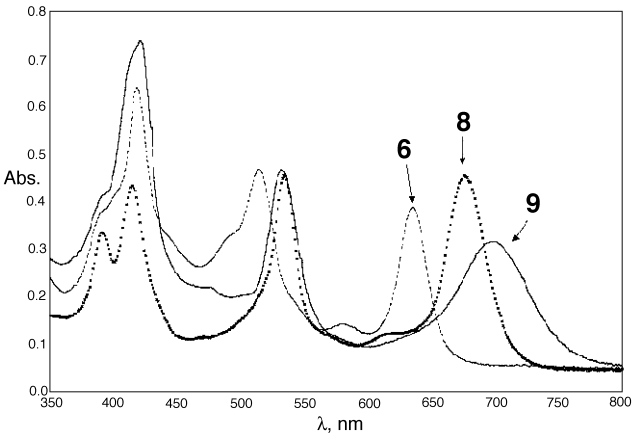

Figure 1. UV–visible spectra of **6**, **8** and **9** in CH_2Cl_2.

dipyrromethene moiety of **6** to yield the BODIPY® complexes was accomplished under basic conditions. Although a similar reaction was carried out by Burgess et al.[24] at higher temperatures (70 °C) using toluene as solvent, the BF_3 complexation took place rapidly at room temperature in 65% yield (Scheme 1). A color change from green to red attested to the fast complexation reaction. The reaction flask was shielded from light and was purged with argon to minimize any decomposition of the dipyrromethenoporphyrin. The corresponding BF_2 complex was stable under the same conditions. The free base (M=2H) fused dipyrromethenoporphyrin **11** and its BF_2 complex **12** were synthesized from the copper dipyrromethenoporphyrin **8** (Scheme 2). The copper dipyrromethenoporphyrin **8** was demetalated with 2% H_2SO_4 in TFA to give the free base dipyrromethenoporphyrin **11** which was unstable and prone to decomposition upon exposure to light and air. The instability of the metal-free dipyrromethenoporphyrin **11** caused its synthesis from the corresponding free base formyl-pyrroloporphyrin to be unsuccessful. The zinc dipyrromethenoporphyrin BF_2 complex **13** was synthesized by metalation with $Zn(OAc)_2$ in toluene in 68% yield (Scheme 2).

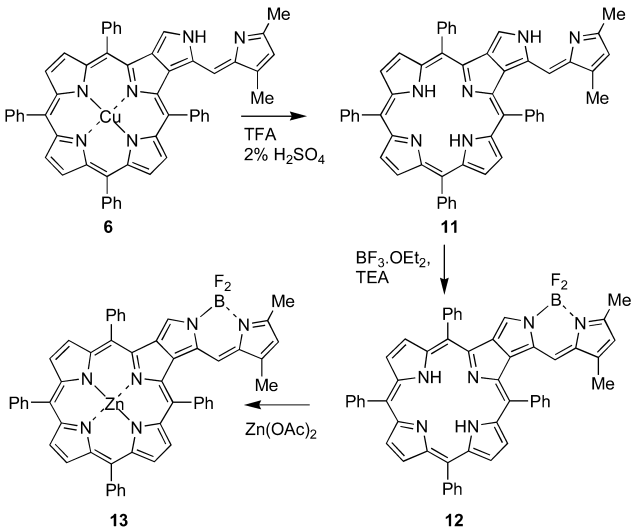

Scheme 2. Synthesis of ZnTPP-BODIPY® **13**.

3.2. Photophysical properties

The absorption spectra of **12** and **13** show three quite intense bands in the 300–750 nm region (Table 1 and Fig. 2). The same behavior is observed for the Cu complex **8**. These spectra are different from those expected by the addition of the spectra of TPP and of BODIPY® units. In particular, in the region around 400 nm, **8**, **12** and **13** present a structured transition with a molar absorption coefficient much lower than that typically observed in this spectral region for TPPs. At longer wavelengths, two transitions with similar intensities are present with energies and absorption coefficients only slightly dependent upon metalation. On the contrary, while BODIPY® units have a narrow transition whose energy is related to its substituents, typically with $\varepsilon \approx 100{,}000\ M^{-1}\ cm^{-1}$, the TPPs present in this region a set of Q-bands, less intense and more strongly dependent upon metalation.

Table 1. Photophysical data in CH_2Cl_2 of the porphyrin-BODIPY® systems studied

Compound	λ_{max} (nm)	ε ($M^{-1}\ cm^{-1}$)	λ_{max} (nm)	τ (ns)	Φ
8	390	53,000	–	–	–
	412	72,200			
	531	78,300			
	675	80,000			
9	410	10,600	–	–	–
	529	78,900			
	695	60,300			
11	393	55,200	690	7.0	0.076
	425	41,000			
	529	53,000			
	598	27,200			
	631	28,600			
	680	18,500			
12	388	51,500	693	4.2	0.04
	413	44,500			
	531	65,000			
	640	58,250			
13	392	55,000	714	1.6	0.053
	415	64,000			
	539	80,500			
	676	61,000			

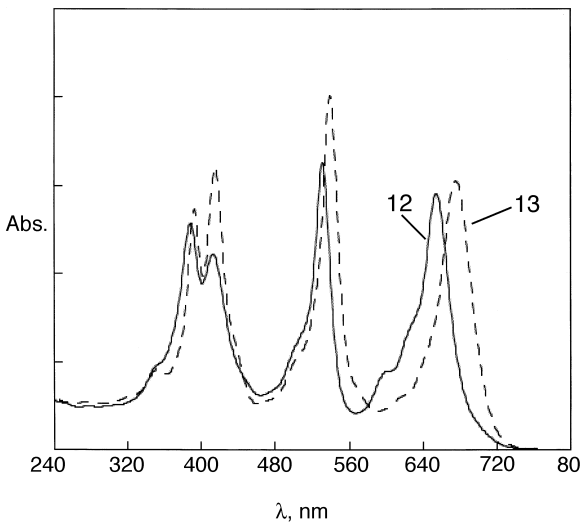

Figure 2. Absorption spectrum of **12** and **13** (dashed line) in CH_2Cl_2 at room temperature.

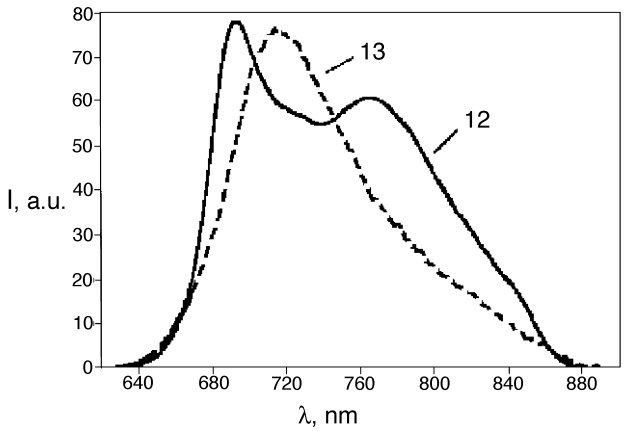

Figure 3. Fluorescence spectrum of **12** and **13** (dashed line) in CH_2Cl_2 at room temperature.

It is interesting to note that, while for porphyrins on going from the free base to their Zn complexes an increase of the energy of the lowest transition is observed, the reverse behavior is encountered on going from **12** to **13**. The same pattern is observed in the luminescence spectra (Fig. 3 and Table 1), where **12** and **13** show a fluorescence band in the region around 700 nm.

The excitation spectra strictly match the absorption analogs, indicating that excitation over all the 240–700 nm region leads to the population of the fluorescent excited state with unitary efficiency, independently of the nature of the chromophore involved in the absorption process. The low Stokes-shift observed between the lowest absorption and the fluorescence band indicates that the distortion occurring in going from the ground state to the fluorescent excited state is also low, suggesting a small charge transfer character in the latter state. It should be noted that the fluorescence quantum yields observed, although not very high, are still of interest because of their spectral location; new fluorescent labels and sensors in the near IR region are of great interest for biological and biotechnological applications. Compounds **6** and **8**, did not show any fluorescence band both at room temperature and at 77 K ($\Phi < 10^{-5}$).

For all the compounds studied, no phosphorescence was observed even at 77 K; we believe it to lie in a region outside the instrumental range (900 nm being the upper limit).

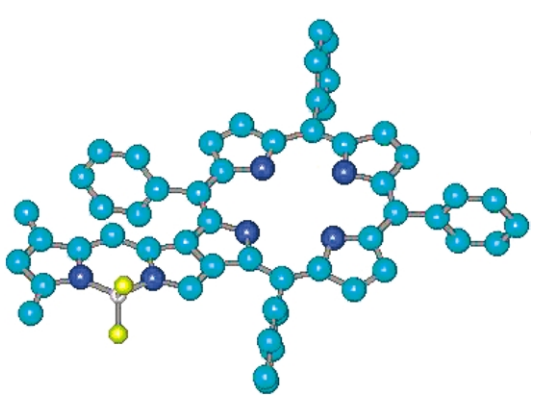

Figure 4. PM3 optimized geometry of **12**. Hydrogen atoms are not shown.

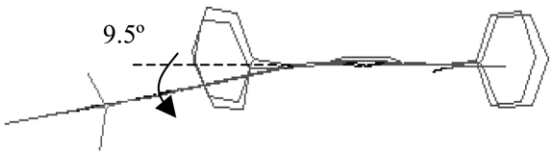

Figure 5. View of **12** showing the angle between the H_2TPP and BODIPY® units.

3.3. Optical properties

To further investigate the optical properties of the TPP-BODIPY® species we performed semi-empirical Hartree–Fock calculations. Starting from a planar configuration, we optimized the geometry of **12** by using the PM3 method.[25] The optimized geometry configuration is shown in Figure 4. This structure is not planar (Fig. 5) and an angle of 9.5° is found between the H_2TPP ring and the BODIPY® moiety; furthermore the H_2TPP macrocycle presents some deviations from planarity. These results are in good accord with features observed in the X-ray structure of the similar dipyrromethanoporphyrin **14**.[15b]

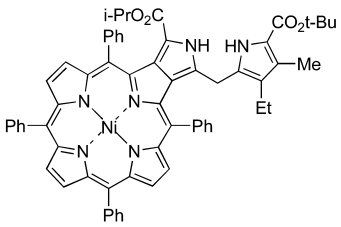

14

Optical properties of **12**, in the optimized geometry, were obtained by using the intermediate neglect diatomic overlap/spectroscopic parametrization (INDO/S) method[26] followed by a converged configuration interaction (CIS). In the CIS calculation, we considered only single excitations from the highest occupied molecular orbitals of **12** to the lowest unoccupied molecular orbitals. Figure 6 shows the calculated absorption spectrum for **12**. Here, an arbitrary Gaussian broadening of the transition energies has been used and no vibronic replicas have been included. A remarkably good agreement with experimental data is found. The minor blue-shift of the calculated absorption peaks with respect to the measured ones is typical of INDO/SCI calculations.[27] The calculated absorption spectrum of **12** also shows a large decrease in the molar absorpion coefficient of the Soret band with respect to the H_2TPP molecule, as observed in the experimental spectrum.

In order to understand the features of the calculated spectrum, we also report (in Fig. 6) the absorption spectra of the separate H_2TPP and BODIPY® fragments as obtained from the optimized geometry of **12** (that is, keeping the geometry calculated for **12**). The H_2TPP and BODIPY® fragments, even in this slightly distorted geometry, present absorption peaks similar to those of the isolated molecules and consequently the presence of a distortion in **12** is not responsible for the appearance of the low energy (640 nm) absorption peak. The appearance of the low energy absorption peak is mainly due to the increased extension of the π-conjugation along the entire molecule. This is

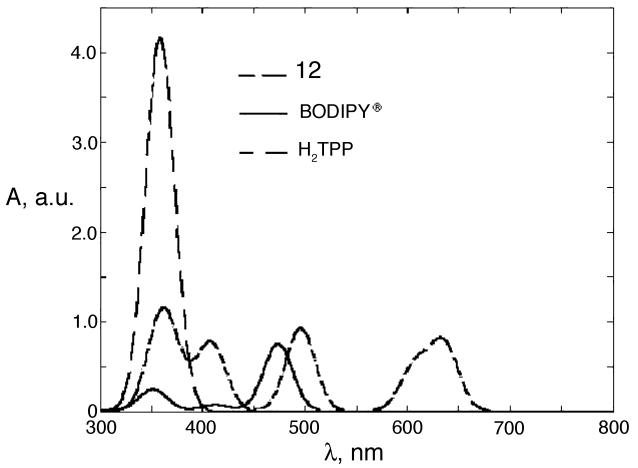

Figure 6. Calculated absorption spectra of **12** and of the separate TPP and BODIPY® molecules in the optimized geometry for **12**. An artificial broadening of the levels has been considered in order to better compare with experimental results.

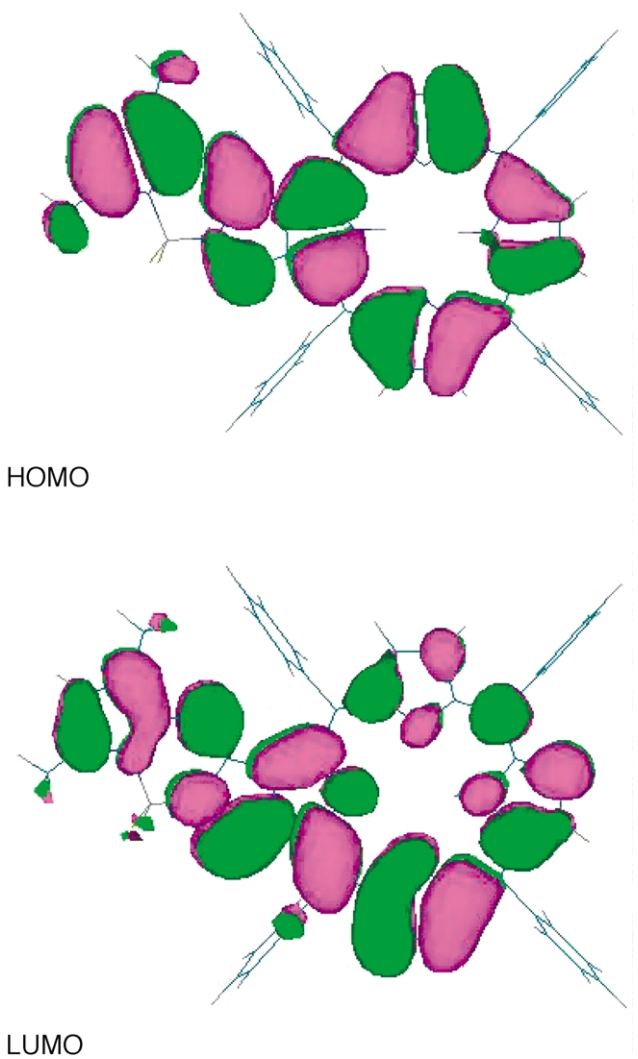

Figure 7. Calculated HOMO and LUMO wavefunctions for **12**. The INDO/S method was used, assuming a PM3 optimized geometry.

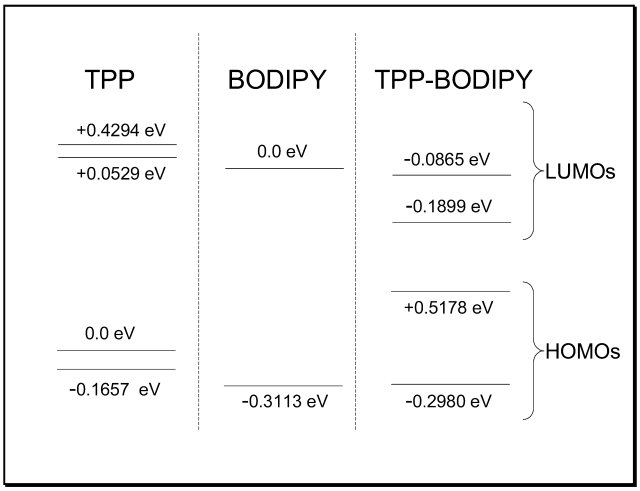

Figure 8. HOMO and LUMO energy levels for **12** and for the isolated H_2TPP and BODIPY® molecules. In order to emphasize the energy difference between levels we set the zero of the energy for LUMO levels with that of the BODIPY® LUMO, while for HOMO levels the zero energy is the TTP HOMO.

shown in Figure 7, in which we plot the HOMO and LUMO of **12**.

Clearly, the HOMO/LUMO wavefunctions extend over the entire complex. In Figure 8, we report the calculated levels for isolated H_2TPP and BODIPY® molecules and also for **12**. HOMO as well as LUMO levels of H_2TPP and BODIPY® are very close in energy (within 0.31 eV for the HOMOs and within 0.087 eV for the LUMOs), which results in a strong interaction between these orbitals. This interaction pushes the HOMO level of **12** toward higher energy while the LUMO level is pushed toward lower energies. This leads to an overall reduction of the HOMO–LUMO gap of **12** with respect to that of the isolated molecules. Indeed, a close inspection of the excited states reveals that the lowest excited state of **12** (640 nm) is mainly composed by the HOMO and LUMO levels which are completely delocalized along the entire molecule. Similar behavior was observed for β-fused oligoporphyrin system where the extension of the π-conjugation resulted in the appearance of a low energy peak around 700 nm.[6] The comparison between **11** and **12** is shown in Figure 9. Again

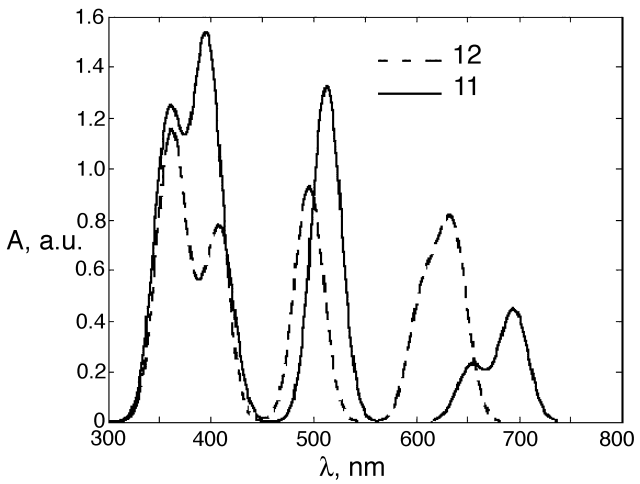

Figure 9. Calculated absorption spectra of **11** and **12** (dashed line).

there is a good accord with the experimental observation that the absence of the BF_2 group increases the intensity of the high energy absorption peaks while the low energy one is reduced.

3.4. Conclusions

Synthetic methodology has been developed for the preparation of dyes in which a porphyrin macrocycle is directly fused to a BODIPY® moiety through two β-pyrrolic carbons. The optical spectra of the resulting dyads show bands in the 300–750 nm region, and characterized by a reduction of the absorbance of the Soret band and the presence of an absorption band of similar intensity around 650 nm. A fluorescence band was observed in the region around 700 nm, with a low Stokes-shift observed between the lowest absorption and the fluorescence band. This behavior is different from the linear superimposition of the spectra of isolated components of the dyad and cannot be ascribed to deformation of the molecular skeleton of both moieties. To obtain further information on the origin of these optical features, we carried out a INDO/SCI calculation on **12**. These studies showed that the optical properties of **12** derived from an increased extension of the π-conjugation along the entire molecule.

Acknowledgements

Support from CNR-MADESS II (Italy), the University of Bologna (Funds for Selected Topics, Italy) and from the US National Science Foundation (CHE-02-96012) is gratefully acknowledged.

References and notes

1. Shirakawa, H.; Louis, E. J.; MacDiarmid, A. G.; Chiang, C. K.; Heeger, A. J. *Chem. Commun.* **1977**, 578.
2. (a) Metzger, R. M. *Acc. Chem. Res.* **1999**, *32*, 950. (b) Würthner, F. *Angew. Chem. Int. Ed.* **2001**, *40*, 1037. (c) Vilan, A.; Cahen, D. *Trends Biotechnol.* **2002**, *20*, 22, and references therein.
3. Kraft, A. *Chem. Phys. Chem.* **2001**, *2*, 163.
4. Tsuda, A.; Osuka, H. *Science* **2001**, *293*, 79.
5. *The Porphyrin Handbook*; Kadish, K. M., Smith, K. M., Guilard, R., Eds.; Academic: Boston, MA, 2000.
6. (a) Vicente, M. G. H.; Jaquinod, L.; Smith, K. M. *Chem. Commun.* **1999**, 1771. (b) Paolesse, R.; Jaquinod, L.; Della Sala, F.; Nurco, D. J.; Prodi, L.; Montalti, M.; D'Amico, A.; Di Carlo, A.; Lugli, P.; Smith, K. M. *J. Am. Chem. Soc.* **2000**, *122*, 11295.
7. (a) Lu, T. X.; Reimers, J. R.; Crossley, M. J.; Hush, N. S. *J. Phys. Chem.* **1994**, *98*, 11878. (b) Reimers, J. R.; Lü, T. X.; Crossley, M. J.; Hush, N. S. *Chem. Phys. Lett.* **1996**, *256*, 353. (c) Reimers, J. R.; Hall, L. E.; Crossley, M. J.; Hush, N. S. *J. Phys. Chem. A* **1999**, *103*, 4385.
8. Wang, H. J. H.; Jaquinod, L.; Nurco, D. J.; Vicente, M. G. H.; Smith, K. M. *Chem. Commun.* **2001**, 2646.
9. (a) Haugland, R.P.; Kang, H.C. Chemically Reactive Dipyrrometheneboron Difluoride Dyes. U.S. Patent 4,774,339, 1988.(b) Molecular Probes Inc., Eugene, OR.

10. Treibs, A.; Kreuzer, F.-H. *Liebigs Ann. Chem.* **1968**, *718*, 203.
11. Rurack, K.; Kollmannsberger, M.; Daub, J. *Angew. Chem. Int. Ed.* **2001**, *40*, 385.
12. Wada, M.; Ito, S.; Uno, H.; Murashima, T.; Ono, N.; Urano, T.; Urano, Y. *Tetrahedron Lett.* **2001**, *42*, 6711.
13. Li, F.; Yang, S. I.; Ciringh, Y.; Seth, J.; Martin, C. H., III; Singh, D. L.; Kim, D.; Birge, R. R.; Bocian, D. F.; Holten, D.; Lindsey, J. S. *J. Am. Chem. Soc.* **1998**, *120*, 10001.
14. Kumaresan, D.; Agarwal, N.; Gupta, I.; Ravikanth, M. *Tetrahedron* **2002**, *58*, 5347.
15. (a) Jaquinod, L.; Gros, C.; Olmstead, M. M.; Antolovich, M.; Smith, K. M. *Chem. Commun.* **1996**, 1475. (b) Gros, C. P.; Jaquinod, L.; Khoury, R. G.; Olmstead, M. M.; Smith, K. M. *J. Porphyrins Phthalocyanines* **1997**, *1*, 201.
16. Smith, K. M. In *Porphyrins and Metalloporphyrins*; Smith, K. M., Ed.; Elsevier: Amsterdam, 1975.
17. Shea, K. M.; Jaquinod, L.; Smith, K. M. *J. Org. Chem.* **1998**, *63*, 7013.
18. Seybold, P. G.; Gouterman, M. *J. Mol. Spectrosc.* **1969**, *31*, 1.
19. Credi, A.; Prodi, L. *Spectrochim. Acta, A* **1998**, *54*, 159.
20. Jaquinod, L. *The Porphyrin Handbook*; Kadish, K. M., Smith, K. M., Guilard, R., Eds.; Academic: Boston, MA, 2000; Vol. 1, p 201.
21. Tardieux, C.; Bolze, F.; Gros, C. P.; Guilard, R. *Synthesis* **1998**, 267.
22. Clezy, P. S.; Fookes, C. J. R.; Liepa, A. J. *Aust. J. Chem.* **1972**, *25*, 1979.
23. Montforts, F.; Scheurich, G.; Meier, A.; Haake, G.; Hoper, F. *Tetrahedron Lett.* **1991**, *29*, 3477.
24. Burghart, A.; Kim, H.; Welch, M.; Thoresen, L. H.; Reibenspies, J.; Burgess, K. *J. Org. Chem.* **1999**, *64*, 7813.
25. Stewart, J. J. *J. Comput. Chem.* **1989**, *10*, 221.
26. (a) Ridley, J. E.; Zerner, M. C. *Theor. Chem. Acta* **1973**, *32*, 111. (b) Ridley, J. E.; Zerner, M. C. *Theor. Chem. Acta* **1976**, *42*, 223.
27. (a) Gigli, G.; Lomascolo, M.; Cingolani, R.; Barbarella, G.; Zambianchi, Z.; Antolini, L.; Della Sala, F.; Di Carlo, A.; Lugli, P. *Appl. Phys. Lett.* **1998**, *73*, 2414. (b) Rawlings, D. C.; Davidson, E. R.; Gouterman, M. *Theor. Chim. Acta* **1982**, *61*, 227. (c) Baker, J. D.; Zerner, M. C. *Chem. Phys. Lett.* **1990**, *175*, 192.